Bioorganic & Medicinal Chemistry xxx (2013) xxx–xxx

Contents lists available at SciVerse ScienceDirect

Bioorganic & Medicinal Chemistry

journal homepage: www.elsevier.com/locate/bmc

Design, synthesis and anti-tuberculosis activity of 1-adamantyl-3-heteroaryl ureas with improved in vitro pharmacokinetic properties

E. Jeffrey North [a], Michael S. Scherman [b], David F. Bruhn [a], Jerrod S. Scarborough [a], Marcus M. Maddox [a], Victoria Jones [b], Anna Grzegorzewicz [b], Lei Yang [a], Tamara Hess [b], Christophe Morisseau [c], Mary Jackson [b], Michael R. McNeil [b], Richard E. Lee [a,*]

[a] Department of Chemical Biology and Therapeutics, St. Jude Children's Research Hospital, 262 Danny Thomas Place, Mail Stop 1000, Memphis, TN 38105, USA
[b] Mycobacteria Research Laboratories, Department of Microbiology, Immunology and Pathology, Colorado State University, Fort Collins, CO 80523, USA
[c] Department of Entomology and UC Davis Comprehensive Cancer Center, University of California, Davis, CA 95616, USA

ARTICLE INFO

Article history:
Received 31 December 2012
Revised 6 February 2013
Accepted 14 February 2013
Available online xxxx

Keywords:
Tuberculosis
Antimicrobial agents
Transporter
Antibiotics
Medicinal chemistry
MmpL3

ABSTRACT

Out of the prominent global ailments, tuberculosis (TB) is still one of the leading causes of death worldwide due to infectious disease. Development of new drugs that shorten the current tuberculosis treatment time and have activity against drug resistant strains is of utmost importance. Towards these goals we have focused our efforts on developing novel anti-TB compounds with the general structure of 1-adamantyl-3-phenyl urea. This series is active against *Mycobacteria* and previous lead compounds were found to inhibit the membrane transporter MmpL3, the protein responsible for mycolic acid transport across the plasma membrane. However, these compounds suffered from poor in vitro pharmacokinetic (PK) profiles and they have a similar structure/SAR to inhibitors of human soluble epoxide hydrolase (sEH) enzymes. Therefore, in this study the further optimization of this compound class was driven by three factors: (1) to increase selectivity for anti-TB activity over human sEH activity, (2) to optimize PK profiles including solubility and (3) to maintain target inhibition. A new series of 1-adamantyl-3-heteroaryl ureas was designed and synthesized replacing the phenyl substituent of the original series with pyridines, pyrimidines, triazines, oxazoles, isoxazoles, oxadiazoles and pyrazoles. This study produced lead isoxazole, oxadiazole and pyrazole substituted adamantyl ureas with improved in vitro PK profiles, increased selectivity and good anti-TB potencies with sub μg/mL minimum inhibitory concentrations.

1. Introduction

Mycobacterium tuberculosis (*M. tb*) is the pathogen responsible for the infectious disease tuberculosis (TB) which still today is responsible for a vast number of deaths globally.[1] Increasing rates of resistance and inadequacies of current TB chemotherapeutics necessitate the need for new drugs which can potentially shorten the drug treatment, increase patient compliance and have activity against drug resistant strains including multi-drug-resistant (MDR) and extremely drug-resistant (XDR) tuberculosis.

Previously we developed a series of 1-adamantyl-3-phenyl ureas **1**–**6** that had potent anti-tuberculosis activity, however they had undesirable pharmaceutical properties, particularly high lipophilicity and poor solubility (Fig. 1).[2] The biochemical basis for their activity is complex, as it was shown that these compounds inhibited mammalian soluble epoxide hydrolase (sEH) inhibitors[3] and multiple *M. tb* epoxide hydrolases including EphB[2,4] and EphE.[2] However, *M. tb* epoxide hydrolases are individually non-essential. In attempts to rationalize the primary target for anti-tuberculosis activity, we used genetic approaches by generating and sequencing resistant mutants for **1**. We identified a further and essential target for this compound series, the membrane transporter Mmpl3, which is believed to play a major role in exporting mycolates to mycobacterial cell surface.[5] Although our first generation adamantyl ureas possessed potent anti-TB activity,[2] they had two principal issues: (i) they were highly hydrophobic and consequently had poor solubility and high human plasma protein binding (HPPB); (ii) though while highly selective with respect to anti-TB activity compared to cytotoxicity and activity against other bacteria, these compounds still had potent human soluble epoxide hydrolase (sEH) activity which may not be pharmacologically desirable (Fig. 1).[2] Thus the purpose of this study is to design and develop analogs that maintain anti-tuberculosis activity but have improved pharmacokinetic (PK) properties, most notably solubility and selectivity away from human sEH inhibition. In this study we used

* Corresponding author. Tel.: +1 (901) 595 6617; fax: +1 (901) 595 5715.
E-mail address: Richard.lee@stjude.org (R.E. Lee).

0968-0896/$ - see front matter © 2013 Elsevier Ltd. All rights reserved.
http://dx.doi.org/10.1016/j.bmc.2013.02.028

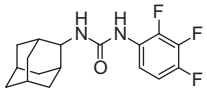

1

MIC = 0.01 μg/mL
Human sEH IC_{50} = 0.4 nM
ClogP = 5.1
Solubility < 0.1 μg/mL
HPPB = 98.8%

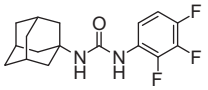

2

MIC = 0.4μg/mL
Human sEH IC_{50} = 0.4 nM
ClogP = 4.0
Solubility < 0.1 μg/mL

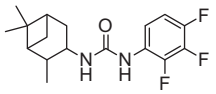

3

MIC = 0.02 μg/mL
Human sEH IC_{50} = 0.4 nM
ClogP = 5.2
Solubility < 0.1 μg/mL
HPPB = 99.2%

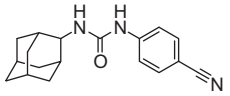

4

MIC = 0.4 μg/mL
Human sEH IC_{50} = 1.1 nM
ClogP = 4.9
Solubility < 0.1 μg/mL
HPPB = 99.0%

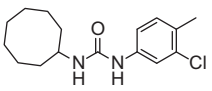

5

MIC = 0.01 μg/mL
Human sEH IC_{50} = 0.4 nM
ClogP = 5.8
Solubility < 0.1 μg/mL
HPPB = 99.7%

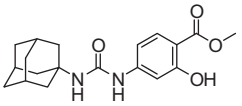

6

MIC = 0.4 μg/mL
Human sEH IC_{50} = 1.2 nM
ClogP = 4.1
Solubility = 0.51 μg/mL
HPPB = 96.9%

Figure 1. Previously synthesized adamantyl–phenyl ureas **1–6** with *M. tb* H37Rv MIC values, human sEH IC_{50} values, *c*Log*P* values, solubility and human protein plasma binding (HPPB).[2]

rational bioisosteric replacements for the phenyl group of the first generation urea in six miniseries (arylsulfonamides, pyridines, isoxazoles, thiazoles, oxadiazoles and pyrazoles) in order to increase polarity, which should help increase solubility and lower HPPB, while maintaining good anti-tuberculosis activity and potentially decreasing affinity to human sEH.

2. Results and discussion

2.1. Chemistry and SAR of adamantyl–heteroaryl ureas

2.1.1. Series 1 – Sulfonamides

One approach to boost the solubility of this series is to introduce an ionizable group in the para position of the phenyl ring which has been previously shown to be tolerated.[2,6] One such function group is found in sulfonamide antibiotics, which were historically optimized by the addition of an electron deficient outer ring to ionize the sulfonamide functionality at physiological pH (Fig. 2).[7] Though the addition of an adamantyl urea to the aniline position of the sulfonamides will block their nascent antimicrobial activity through dihydropteroate synthase inhibition,[8] incorporation of the sulfonamide scaffold to the urea scaffold appeared to match the preexisting SAR or our anti-TB indication.[2] Thus, the adamantyl–phenylsulfonamide ureas were rapidly synthesized using microwave heating at 200 °C for 10 min from common sulfonamide antibiotics and 1-adamantyl isocyanate in the presence of triethylamine (Scheme 1).

As desired, all the adamantyl sulfonamides did have increased solubility (10 to 100-fold) over the first generation adamantyl phenyl ureas (Table 1). Despite having improved solubility (acceptable solubility >10 μg/mL), all the adamantyl sulfonamides, except **13**, had a large reduction in *M. tb* minimum inhibitory concentration (MIC) compared to **1** (Table 1 and Fig. 1) using microbroth dilution MIC method.[9,10] This suggests that acidic sulfonamide functionalities are not tolerated well by the molecular target or for tubercular entry and are thus detrimental to anti-TB activity. This observation was further validated with **13**, which did possess anti-TB activity (6.25 μg/mL) and contained a non-acidic sulfone rather than an acidic aryl sulfonamide found in the other compounds in this series.

2.1.2. Series 2 – N-substituted heterocycles

Another common approach to increase solubility of phenyl rings is the introduction of a heteroatoms resulting in bioisosteric rings such as pyridyl, which may also have the benefit of being more resistant to cytochrome mediated metabolism.[11,12] Thus, pyridine and pyridine analogs (pyrimidine and triazine) were introduced into the adamantyl ureas according to Scheme 2. Predetermining the *c*Log*P* values for each molecule ensured they stayed below our initial lead compound **1** (*c*Log*P* = 5.08) as a computational correlate of solubility. Two different methods were employed to synthesize this series. First, 1-adamantyl isocyanate and heteroarylamine were reacted in the presence of triethylamine in THF. If after four days of heated stirring, little to no product was detected by TLC, method B was used to synthesize the adamantyl heteroaryl urea (Scheme 2). Method B utilized butyl lithium to activate the heteroarylamine followed by addition of 1-adamantyl isocyanate.

All pyridines, pyrimidines and triazines had relatively poor anti-TB activity with **15** (3-pyridinyl) having the most potent MIC at 12.5 μg/mL (Table 2). Generally, this series had solubility values at approximately 7 μg/mL, which was not as high as the average solubility of the sulfonamide series, but superior to the initial adamantyl–phenyl leads **1**–**6**. Anti-TB activity for the whole series was inferior to **1**–**6** with the 3-pyridinyl (**15**, MIC = 12.5 μg/mL) showing the best activity which greatly decreased with the 2-pyridinyl substitution (**16**, MIC = 200 μg/mL). Introduction of a second nitrogen in the 2-pyrimidinyl analog (**17**) did not prove effective for

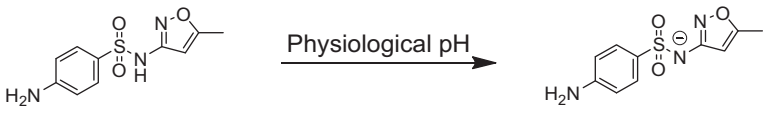

Figure 2. Representation of sulfonamide (sulfamethoxazole) isonization at physiological pH.

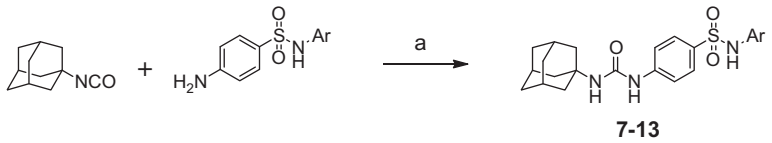

Scheme 1. Synthesis of 1-(1-adamantyl)-3-(benzenesulfonamide)ureas. Reagents and conditions: (a) TEA, THF/DMF (1:1), μw, 200 °C, 10 min.

Table 1
In vitro whole cell anti-TB activity, human sEH inhibition, solubility, and *c*Log*P* of 1-(1-adamantyl)-3-(4-(*N*-(heteroaryl)benzenesulfonamide))ureas

Compd #	Structure	[a]*M. tb* MIC (μg/mL)	[b]Human sEH IC_{50} (nM)	[c]Solubility (μg/mL)	[d]*c*Log*P*
7	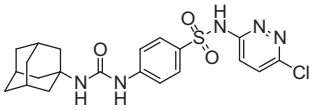	25	19	20.7 ± 0.2	3.6
8	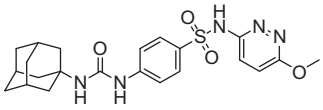	25	7	14.1 ± 1.2	3.4
9	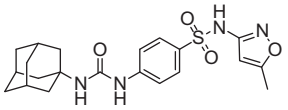	25	292	2.0 ± 0.2	3.4
10	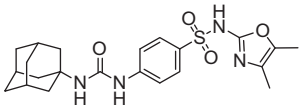	>25	13	27.1 ± 1.4	3.4
11	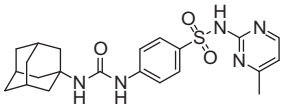	>25	17	2.5 ± 0.1	3.5
12	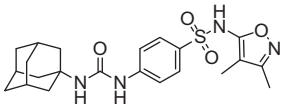	25	31	27.3 ± 0.9	3.1
13	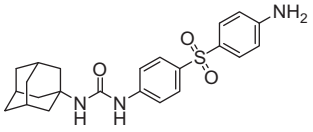	6.25	0.7	0.9 ± 0.1	3.8

[a] In vitro anti-TB activity against *M. tb* H37Rv.
[b] In vitro IC_{50} values against recombinant human sEH (1 nM).
[c] In vitro solubility of ureas in a physiological environment at pH 7.4.
[d] In silico calculation of *c*Log*P* using ChemBioDraw Ultra 12.0.

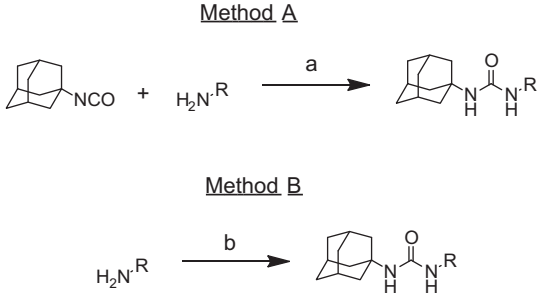

Scheme 2. Synthesis of 1-(1-adamantyl)-3-(heteroaryl)urea. Reagents and conditions: Method A: (a) triethylamine, THF, 70 °C, 4 days; Method B: (b) (i) butyl lithium, THF, −78 °C, 20 min; (ii) 1-adamantyl isocyanate, THF, rt, 1 h.

anti-TB activity, although the 4-pyrimidinyl (**18**) did have the best solubility of this series at 15.5 ± 0.8 μg/mL with modest anti-TB activity at 25 μg/mL. Finally, introduction of a third nitrogen to the ring abolished anti-TB activity completely.

In an attempt to further optimize the solubility of the adamantyl–heteroaryl ureas and obtain potent MIC values, oxazole and isoxazole rings were introduced in the adamantyl–heteroaryl urea scaffold. These compounds were synthesized according to Scheme 2 and summarized in Table 3. The unsubstituted oxazole, **21**, had a more potent MIC value, 6.25 μg/mL, than the unsubstituted isoxazole, **22** (MIC = 50 μg/mL). However, the isoxazole (**22**) had approximately five-times the solubility of the oxazole (**21**). Introduction of a methyl group to the 5-position of the isoxazole ring in **23** increased MIC potency by almost twofold compared to **22**. Increasing the hydrophobicity of the methyl group in **23** to a *t*-butyl group in **24** increased anti-TB activity significantly from a MIC of 27 μg/mL to 1.56 μg/mL. However, solubility dropped by about half from 25.9 ± 1.5 μg/mL with **23** to 11.2 ± 1.6 μg/mL with **24**. Anti-TB activity was abolished with introduction of a bromine to the 'pseudo-ortho' 4-position of the isoxazole ring (**25**,

Table 2
In vitro whole cell anti-TB activity, human sEH inhibition, solubility and *c*Log*P* of 1-(1-adamantyl)-3-pyridinylurea analogs

Compd #	Structure	*M. tb* MIC (μg/mL)	Human sEH IC_{50} (nM)	Solubility (μg/mL)	*c*Log*P*
14	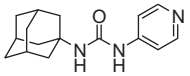	18	174	7.0 ± 0.3	3.2
15	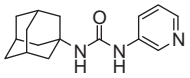	12.5	113	6.7 ± 1.5	3.2
16	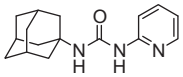	200	1498	1.4 ± 0.2	3.2
17	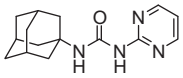	200	24,010	6.9 ± 1.5	2.6
18	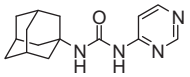	25	775	15.5 ± 0.8	2.6
19	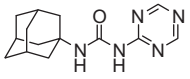	125	79	7.2 ± 0.8	1.8
20	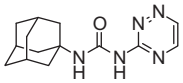	200	1012	6.8 ± 0.3	2.1

Table 3
In vitro whole cell anti-TB activity, human sEH inhibition, solubility and *c*Log*P* of 1-(1-adamantyl)-3-isoxazolylurea analogs

Compd #	Structure	*M. tb* MIC (μg/mL)	Human sEH IC_{50} (nM)	Solubility (μg/mL)	*c*Log*P*
21	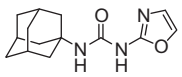	6.25	948	4.4 ± 0.1	2.4
22	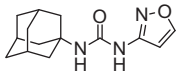	50	46	20.3 ± 1.9	2.7
23	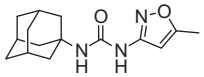	27	136	25.9 ± 1.5	3.0
24	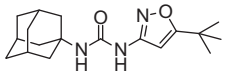	1.56	56	11.2 ± 1.6	4.3
25	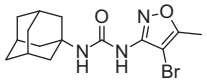	100	0.8	0.1 ± 0.0	3.3
26	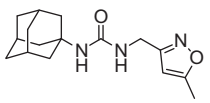	>50	1551	3.0 ± 0.1	2.1
27	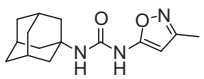	12.5	117	5.5 ± 0.3	3.0
28	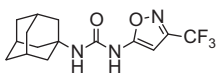	0.78	2	0.77 ± 0.0	3.7
29	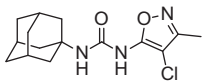	100	0.5	1.5 ± 0.5	3.2
30	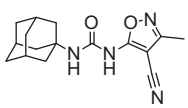	100	25	1.2 ± 0.2	2.8
31	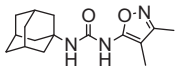	100	20	5.7 ± 2.2	2.6

MIC = 100 μg/mL). Separating the isoxazole ring from the urea functional group by a methylene was detrimental to both anti-TB activity and solubility (**26**, MIC >50 μg/mL, solubility = 3.0 ± 0.1 μg/mL). Switching the oxygen and nitrogen in **23** to the reverse isoxazole in **27** gained a twofold increase in anti-TB activity, however, there was a fivefold reduction in solubility. Increasing the hydrophobicity of the 3-position from methyl (**27**, MIC = 12.5 μg/mL) to trifluoromethyl (**28**, MIC = 0.78 μg/mL) of the reverse isoxazole also significantly increased anti-TB activity. Similarly it was noted previously, introduction of chlorine (**29**), cyano (**30**) or methyl (**31**) into the 'pseudo-ortho' 4-position also abolished anti-TB activity in the reverse isoxazole series, each with MIC = 100 μg/mL. Of note, the oxazole **21** made a significant and desirable improvement with regards to selectivity for anti-TB activity over human sEH activity.

A four compound thiazole series was synthesized to evaluate the role of oxygen over sulfur (Table 4). A twofold increase in anti-TB activity was observed from the oxazole **21** (MIC = 6.25 μg/mL), to the thiazole **32** (MIC = 3.13 μg/mL). Unlike the isoxazole series, anti-TB activity did not increase significantly with the introduction of hydrophobic methyl groups to the 4- and 5-positions of the thiazole ring (**33** and **34**, respectively). However, introduction of a benzathiazole (**35**) significantly improved the MIC value to 0.78 μg/mL from 3.13 μg/mL with **32**. Unfortunately, none of the thiazoles had acceptable solubility with **33** having the highest at 5.0 ± 0.3 μg/mL.

In order to help increase the solubilitiy of the isoxazole series, a more polar oxadiazole ring was evaluated (Table 5). A similar SAR was observed, in that increasing substituent hydrophobicity in the 5-position of the oxadiazole ring increased anti-TB activity. This was observed with **36** (MIC = 25 μg/mL), having a methyl group in the 5-position, and **37** (MIC = 1.56 μg/mL), having an isopropyl group in the 5-position. However, solubility of **36** and **37** were essentially the same at ~10 μg/mL. Anti-TB activity was reduced with the restriction of the isopropyl group to cyclic groups. There was approximately an eightfold reduction for both cyclopropyl (**38**, MIC = 12.5 μg/mL) and cyclobutyl (**39**, MIC = 12.5 μg/mL) and 64-fold reduction for thiophenyl (**40**, MIC = 100 μg/mL) compared to **37**. Interestingly, solubility was increased significantly with the introduction of a cyclopropyl group in the 5-position. It was also noted that the oxadiazole series had lower human sEH activity compared to the previously evaluated series.

With the encouragement that heteroaryl rings can be modified to modulate MIC, solubility and sHE inhibition, a small series of pyrazoles were synthesized to further emphasize our current SAR (Table 6). These compounds were synthesized according to Scheme 2. The most promising compound from this series, with regard to anti-TB activity, was the ethyl substituted pyrazole **43** with an MIC 1.56 μg/mL. Compound **42** achieved the highest selectivity for *M. tb* activity over human sHE inhibition among the pyrazoles. There was an inverse relationship between *M. tb* activity and solubility, with **43** having the most potent anti-TB activity yet the poorest solubility and **44** having the opposite.

It has been observed in previous studies, that, though synthetically less accessible, attachment of the adamantyl group through the adamantyl secondary 2-position, as opposed to the tertiary 1-position, significantly increases anti-TB activity.[2] This was seen in comparing **1** and **2**, where the secondary-linked adamantyl–phenyl urea **1** is 40-fold more potent than **2**, the tertiary-linked adamantyl–phenyl urea (Fig. 1). Therefore, a series of adamantyl–heteroaryl urea analogs, linked through the secondary 2-position on adamantane, using the best heteroaryl ring systems generated thus far were designed. Subsequently, these compounds were synthesized by sequentially reacting a heteroarylamine and 2-adamantylamine with triphosgene in the presence of diisopropylethylamine (Scheme 3 and Table 7). All of the secondary-linked adamantyl–heteroaryl urea analogs had increased or equal solubility compared to the tertiary linked adamantyl–heteroaryl precursors, except for **50** and **52** which had decreased solubility. Encouragingly, the secondary-linked isoxazole **46** had both a 15-fold improvement in MIC (0.10 μg/mL) and 2-fold improvement in solubility (22.7 ± 2.2 μg/mL) over the previous tertiary-linked version (**24**). The contribution to activity of the position of adamantyl linkage on **23**, which has a poor MIC value yet good solubility, was also evaluated. As expected, the secondary-linked compound **47** achieved a fourfold improvement in MIC (6.25 μg/mL) over the tertiary-linked compound **23** (MIC = 27 μg/mL). Of benefit, the solubility went unchanged at ~25 μg/mL. A slightly different SAR was observed for the oxadiazoles. As seen before with the tertiary-linked adamantyl–heteroaryl ureas, constraining the isopropyl side chain to ring systems reduces the MIC values. This is not the case with the secondary-linked adamantyl–heteroaryl ureas, however. Anti-TB activity is slightly reduced when the isopropyl (**49**, MIC = 1.56 μg/mL) side chain is constrained to the cyclopropyl (**50**, MIC = 3.13 μg/mL), yet slightly increased when expanded to the cyclobutyl (**51**, MIC = 0.78 μg/mL). Many compounds in the secondary-linked series, particularly oxadizoles **49** and **50** and pyrazoles **52** and **53**, achieved the highest selectivity for anti-TB activity versus sEH inhibition compared to all other compounds studied in this series.

2.2. ADME-toxicity properties

In order to reveal possible adverse properties of the adamantyl–heteroaryl ureas, we determined the IC_{50} values for compounds with MIC values less than 10 μg/mL against the VERO monkey kidney cell line (Table 8). The majority of adamantyl–heteroaryl ureas

Table 4
In vitro whole cell anti-TB activity, human sEH inhibition, solubility and *c*Log*P* of 1-(1-adamantyl)-3-thiazolylurea analogs

Compd #	Structure	*M. tb* MIC (μg/mL)	Human sEH IC_{50} (nM)	Solubility (μg/mL)	*c*Log*P*
32	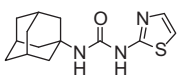	3.13	83	3.2 ± 0.5	3.2
33	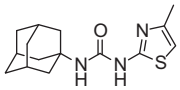	1.56	485	5.0 ± 0.3	3.7
34	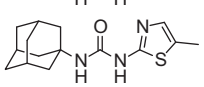	3.13	116	0.1 ± 0.0	3.7
35	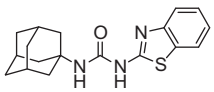	0.78	3	0.5 ± 0.0	4.7

Table 5
In vitro whole cell anti-TB activity, human sEH inhibition, solubility and *c*Log*P* of 1-(1-adamantyl)-3-oxadiazolylurea analogs

Compd #	Structure	*M. tb* MIC (μg/mL)	Human sEH IC_{50} (nM)	Solubility (μg/mL)	*c*Log*P*
36	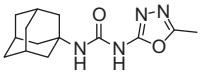	25	595	9.77 ± 1.5	1.9
37	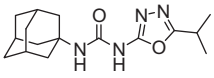	1.56	557	9.54 ± 1.2	2.9
38	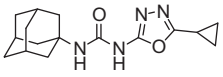	12.5	503	38.3 ± 0.5	2.4
39	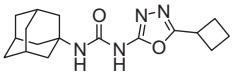	12.5	241	10.5 ± 0.2	2.9
40	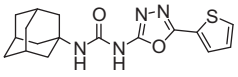	100	1575	2.2 ± 0.1	3.7

Table 6
In vitro whole cell anti-TB activity, human sEH inhibition, solubility and *c*Log*P* of 1-(1-adamantyl)-3-pyrazolylurea analogs

Compd #	Structure	*M. tb* MIC (μg/mL)	Human sEH IC_{50} (nM)	Solubility (μg/mL)	*c*Log*P*
41	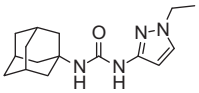	25	884	10.5 ± 0.1	2.9
42	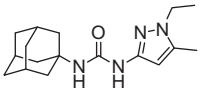	12.5	2512	13.2 ± 2.8	3.2
43	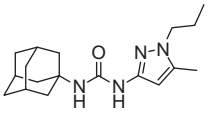	1.56	751	1.43 ± 0.0	3.4
44	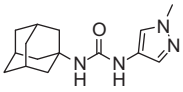	50	488	41.1 ± 2.2	2.4

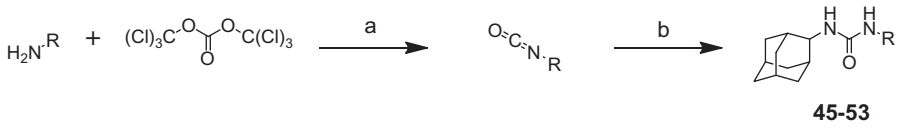

Scheme 3. Synthesis of 1-(2-adamantyl)-3-(aromatic)ureas. Reagents and conditons: (a) DIPEA, DCM, THF, −78 °C, 20 min; (b) DIPEA, DCM, THF, rt, 1 h.

had cytotoxicity IC_{50} values below 50 μg/mL, ranging from 6 to 36 μg/mL. Compounds **13**, **50** and **52** have IC_{50} values greater than 100 μg/mL. Among the 18 compounds tested, 11 of them achieved selectivity indexes greater than 10 showing good therapeutic potential for the adamantyl–heteroaryl ureas. In particular, the adamantyl–heteroaryl ureas linked through the secondary carbon on adamantane.

Further evaluation of lead compounds were performed in 96-well plate-based in vitro PK assays including human plasma protein binding (HPPB), microsomal stability and PAMPA permeability. Table 9 shows the in vitro PK data for the 15 best compounds, each with MIC values less than 3.5 μg/mL. One of the main focuses with the development of adamantyl heteroaryl ureas was to boost the in vitro PK properties properties while maintaining anti-tuberculosis activity. Rapid equilibrium dialysis was used to determine the % binding of the adamantyl ureas to human plasma protein. Traditionally it is believed that only free drug (unbound) is able to elicit its biological response(s), therefore low protein binding is optimal. All of the compounds had relatively high protein binding, with compound **46** having the lowest at 95.2% bound. Incubation of the adamantyl–heteroaryl ureas with mouse liver microsomes was used to monitor the metabolic liability of these compounds to phase I hepatic metabolism. Compounds **24**, **46**, **49** and **51** had microsomal stabilities of 2.2, 1.4, 2.4 and 1.1 h half lives, respectively. Target microsomal stability is typically at least >30% of drug remaining after 90 min, which compounds **24**, **46**, **49** and **51** all achieve. Permeability of these compounds was determined using the parallel artificial membrane permeability assay (PAMPA). Three out of the four lead compounds (**46**, **49** and **51**) all have excellent permeability, having values at least as good as albendazole, our positive control, which has a permeability of approximately 441×10^{-6} cm/s.

Please cite this article in press as: North, E. J.; et al. *Bioorg. Med. Chem.* (2013), http://dx.doi.org/10.1016/j.bmc.2013.02.028

Table 7
In vitro whole cell anti-TB activity, human sEH inhibition, solubility and *c*Log*P* of 1-(2-adamantyl)-3-isoxazolylurea analogs

Compd #	Structure	*M. tb* MIC (μg/mL)	Human sEH IC_{50} (nM)	Solubility (μg/mL)	*c*Log*P*
45	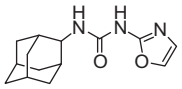	12.5	46	14.9 ± 2.7	3.5
46	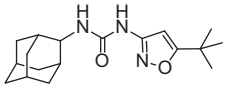	0.10	73	22.7 ± 2.2	5.3
47	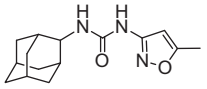	6.25	5	25.5 ± 2.8	4.0
48	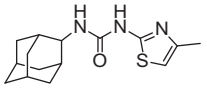	1.56	710	1.5 ± 0.2	4.7
49	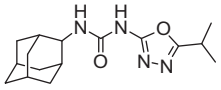	1.56	843	10.1 ± 4.0	3.9
50	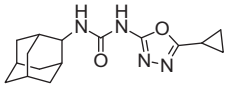	3.13	2408	4.8 ± 2.6	3.4
51	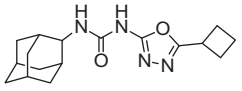	0.78	382	10.3 ± 2.2	4.0
52	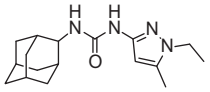	3.13	2463	2.9 ± 0.3	4.2
53	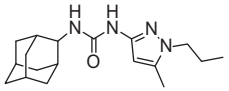	1.56	936	2.0 ± 0.1	4.7

Table 8
In vitro cytotoxicity and selectivity index for key adamantyl urea inhibitors with MIC <10 μg/mL

Compd	[a]Cytotoxicity IC_{50} (μg/mL)	[b]Selectivity index	Compd	[a]Cytotoxicity IC_{50} (μg/mL)	[a]Selectivity index
13	144 ± 6	23	**43**	26 ± 1	17
21	22 ± 7	4	**46**	7 ± 0	70
24	6 ± 0.4	4	**47**	>48	>8
28	24 ± 15	31	**48**	60 ± 1	38
32	22 ± 5	7	**49**	33 ± 5	21
33	13 ± 0	8	**50**	180 ± 14	58
34	23 ± 4	7	**51**	36 ± 6	46
35	17 ± 4	22	**52**	163 ± 25	52
37	11 ± 1	7	**53**	83 ± 1	53

[a] In vitro human mammalian cytotoxicity against VERO cell line.
[b] Selectivity index = cytotoxicity IC_{50}/MIC.

3. Conclusions

Common approaches to optimization the pharmaceutical properties of an initial lipophilic hit, something which is common in anti-tuberculosis drug discovery, include introducing ionizing functional groups, heteroatoms and/or decreasing non-polar moieties. In our efforts to optimize these properties for our lead series, the adamantyl–phenyl ureas **1**–**6**, a bioisosteric replacement strategy was applied to the phenyl ring producing a new series of adamantyl-heteroaromatic ureas. This strategy significantly improved solubility over the first generation adamantyl–phenyl ureas and was also successful in maintaining good anti-TB MIC values for the isoxazole, thiazole, oxadiazole and pyrazole series. However, despite increased solubility, the sulfonamide and pyridine series failed to have substantial activity against *M. tb*. With regard to the isoxazole, oxadiazole and pyrazole series, substitutions with greater nonpolarity increased anti-TB activity while the majority of active compounds maintained solubility above 10 μg/mL. A similar SAR requirement was also observed with regard to substitution of these five-membered ring heterocyles compared to substituted phenyl groups. Substitutions in the 'pseudo-ortho' position was not tolerated with regard to anti-TB activity, which has been seen before with bulky ortho-substituted phenyl groups.[6] While we were able to achieve good anti-TB activity with increased solubility, HPPB was not significantly decreased over first generation adamantyl–phenyl ureas. This is most likely due to the greasy nature of the shared adamantyl urea core. Generally, the most active compounds had acceptable microsomal stability half-lives and excellent PAMPA permeability but all compounds have high levels of protein binding. Our compounds appear to be specific to *M. tb* and did not possess activity against many gram-positive and gram-negative pathogens, including *Staphylococcus aureus*, *Strepto-*

Please cite this article in press as: North, E. J.; et al. *Bioorg. Med. Chem.* (2013), http://dx.doi.org/10.1016/j.bmc.2013.02.028

Table 9
In vitro pharmacokinetic data for adamantyl urea inhibitors with MIC <3.5 μg/mL

Compd	[a]HPPB (% bound)	[b]Microsomal stability ($t_{1/2}$ = h)	[c]Permeability ($\times 10^{-6}$ cm/s)
24	99.8 ± 0.3	2.2 ± 0.1	[d]nd
28	99.6 ± 0.0	1.4 ± 0.0	nd
32	99.1 ± 0.2	1.0 ± 0.1	543 ± 92
33	99.7 ± 0.0	0.6 ± 0.0	766 ± 35
34	99.8 ± 0.0	0.5 ± 0.0	30 ± 7
35	99.8 ± 0.1	1.9 ± 0.0	nd
37	99.3 ± 0.1	1.7 ± 0.1	333 ± 73
43	99.0 ± 0.1	0.9 ± 0.1	811 ± 212
46	95.2 ± 0.8	1.4 ± 0.0	1157 ± 292
48	99.3 ± 0.1	0.5 ± 0.0	696 ± 41
49	98.0 ± 0.2	2.4 ± 0.2	484 ± 22
50	97.7 ± 0.1	2.0 ± 0.1	860 ± 70
51	98.7 ± 0.2	1.1 ± 0.1	843 ± 77
52	98.1 ± 0.1	1.0 ± 0.1	989 ± 38
53	98.9 ± 0.2	1.7 ± 0.2	398 ± 151

[a] In vitro human plasma protein binding.
[b] In vitro half-life of adamantyl urea in mouse liver microsomes.
[c] In vitro permeability of adamantyl ureas across an artificial membrane (PAMPA).
[d] nd = not determined.

coccus pyogenes, *Streptococcus pneumoniae*, *Bacillus subtilis*, *Acinetobacter*, *Klebsiella pneumoniae* and *Pseudomonas aeruginosa* (see Supplementary data Tables S1 and S2). Activity of the analogs was confirmed as on target against MmpL3 as **46** and **51** caused the same increase in trehalose monomycolate (TMM) and decrease in trehalose dimycolate (TDM) and cell wall bound mycolates as the seen by **1**,[5] (Supplementary data Fig. S1) and by cross resistance testing of **46** and **51** against the *M. tuberculosis* strains resistant to **1** (as described in Ref. 5).

The adamantyl urea pharmacophore has been well studied in the field of human sEH. Human sEH is involved in removing epoxides, a reactive oxygen species.[3] Interestingly, sEH inhibition has been shown to have an anti-inflammatory response and possess potential benefits for many diseases, including high blood pressure and kidney failure.[3] While designing the adamantyl–heteroaryl ureas, it was hoped to achieve selectivity for anti-TB activity over sEH inhibition, and we were overall successful at reducing potency against the human sEH by at least 10 to 100-fold. However, sEH inhibition is not implicated in any foreseen negative side effects and in this study we produced compounds with varying selectivity in this regard. The sulfonamide series had poor *M. tb* activity, yet they had excellent sEH IC_{50} values, with the majority of sulfonamides having <20 nM potencies. Coupled with the fact that sulfonamides had generally good solubility values, these compounds may have the potential to be repurposed as human sEH inhibitors. We were successful in being able to separate good anti-TB activity from sEH inhibition most notably through the introduction of oxadiazole and pyrazole heterocylcles to the adamantyl–heteroaryl ureas. The high therapeutic indices of the adamantyl–heteroaryl ureas suggest they will produce good safety profiles in vivo, which will be further evaluated as the lead compounds are progressed forward towards development in future studies, particularly if problems of high serum protein binding can be addressed.

4. Experimental

4.1. Materials and instrumentation

All chemicals and solvents were purchased from commercial sources. All solvents were dried over desiccant and stored under an argon atmosphere. The chemical reactions were tracked by TLC using Silicycle Silica Gel $60F_{254}$ plates and spots were visualized by UV lamp or I_2 condensation. A Biotage (Charlotte, NC) Initiator microwave was used for all microwave assisted reactions. Melting points were determined using an Optimelt Automated Melting Point System (Stanford Research Systems) and were uncorrected. Compounds were purified using either a Biotage SP silica gel or C18 column on a Biotage Isolera One. ^{1}H NMR were recorded on a 400 MHz Bruker NMR and chemical shifts were reported relative to solvent peak. Analytical RP-HPLC was determined on a Waters Acquity UPLC system equipped with an Acquity BEH C18 column (1.7 μm), flow rate of 0.5 mL/min and a gradient of solvent A (water with 0.1% formic acid) and solvent B (acetonitrile with 0.1% formic acid): 0–0.25 min 97% A; 0.25–3.0 min 3–100% B (linear gradient); 3.0–4.5 min 100% B; 4.5–4.75 min 0–97% A (linear gradient); 4.75–5.0 min 97% A. Both UV absorbance (monitored at 225–475 nm) and ELSD were used as detection methods. All compounds were found to have >95% purity with the described analytical methods. HRMS was determined on a Waters XEVO QTOF LCMS. Cytotoxicity readout was performed on a BioTek Synergy HT (BioTek, Winooski, VT). For solubility and permeability assays, compound quantification was performed on a Biomek FX ADME-TOX workstation (Beckman Coulter Inc., Fullerton, CA). For plasma protein binding and microsomal stability assays, compound quantification was performed on a Waters Acquity UPLC system equipped with an Acquity BEH C18 column (1.7 μm) flow rate of 1.0 mL/min and a gradient of solvent A (water with 0.1% formic acid) and solvent B (acetonitrile with 0.1% formic acid): 0–0.2 min 10–30% B (linear gradient); 0.2–1.6 min 30–95% B (linear gradient); 1.6–1.95 min 95% B; 1.95–2 min 5–90% A (linear gradient).

4.2. General method for adamantyl sulfonamide ureas

1-Adamantyl isocyanate (177 mg, 1.0 mmol), 4-aminosulfonamide (1.2 mmol) and triethylamine (502 μL, 3.6 mmol) were dissolved in a 1:1 mixture of THF/DMF (5 mL) in a microwave safe tube and stirred at 200 °C for 10 min. The solvents were removed under reduced pressure and the crude residue was purified by reverse-phase flash column chromatography using a 0.1% formic acid in water to 0.1% formic acid in acetonitrile gradient.

4.2.1. 1-(1-Adamantyl)-3-(4-(*N*-(6-chloropyridazin-3-yl)benzenesulfonamide))urea (7)

73 mg (15.8%) as a yellow solid; MP = 190–200 °C; ^{1}H NMR (DMSO-d_6) δ = 1.63 (br, 6H), 1.85 (br, 1H), 1.93 (br, 5H), 2.03 (br,

3H), 3.46 (s, 1H), 6.05 (s, 1H), 7.49 (d, J = 8 Hz, 2H), 7.75 (d, J = 8 Hz, 2H), 8.73 (s, 1H); ESI-HRMS: $[M-H]^-$ calcd for $C_{21}H_{23}ClN_5O_3S$: 460.1210, found: 460.1212.

4.2.2. 1-(1-Adamantyl)-3-(4-(*N*-(6-methoxypyridazin-3-yl) benzenesulfonamide))urea (8)

70 mg (15.3%) as a yellow solid; MP = 241–246 °C; ^{1}H NMR (DMSO-d_6) δ = 1.63 (br, 6H), 1.92 (br, 6H), 2.03 (br, 3H), 3.85 (s, 3H), 5.23 (s, 1H), 6.02 (s, 1H), 7.46 (d, J = 8 Hz, 2H), 7.67 (d, J = 8 Hz, 2H), 8.66 (s, 1H); ESI-HRMS: $[M-H]^-$ calcd for $C_{22}H_{26}N_5O_4S$: 456.1706, found: 456.1701.

4.2.3. 1-(1-Adamantyl)-3-(4-(*N*-(5-methylisoxazol-3-yl) benzenesulfonamide))urea (9)

69 mg (16.0%) as a white solid; MP = 235–238 °C; ^{1}H NMR (DMSO-d_6) δ = 1.63 (br, 6H), 1.93 (br, 6H), 2.03 (br, 3H), 2.29 (s, 3H), 6.07 (s, 1H), 6.11 (s, 1H), 7.51 (d, J = 8 Hz, 2H), 7.68 (d, J = 8 Hz, 2H), 8.75 (s, 1H), 11.20 (s, 1H); ESI-HRMS: $[M-H]^-$ calcd for $C_{21}H_{25}N_4O_4S$: 429.1597, found: 429.1595.

4.2.4. 1-(1-Adamantyl)-3-(4-(*N*-(4,5-dimethyloxazol-2-yl) benzenesulfonamide))urea (10)

11 mg (5.0%) as a white solid; MP = 215–218 °C; ^{1}H NMR (DMSO-d_6) δ = 1.64 (br, 6H), 1.83–1.96 (m, 9H), 2.00–2.07 (m, 6H), 6.01 (s, 1H), 7.43 (d, J = 8 Hz, 2H), 7.67 (d, J = 8 Hz, 2H), 8.61 (s, 1H); ESI-HRMS: $[M+H]^+$ calcd for $C_{22}H_{27}N_4O_4S$: 445.1910, found: 445.1945.

4.2.5. 1-(1-Adamantyl)-3-(4-(*N*-(4-methylpyrimidin-2-yl) benzenesulfonamide))urea (11)

20 mg (4.5%) as a white solid; MP = 130–135 °C; ^{1}H NMR (DMSO-d_6) δ = 1.63 (br, 6H), 1.92 (br, 6H), 2.03 (br, 3H), 2.74 (s, 3H), 5.23 (s, 1H), 6.04 (s, 1H), 6.88 (d, J = 8 Hz, 1H), 7.47 (d, J = 8 Hz, 2H), 7.81 (d, J = 8 Hz, 2H), 8.30 (d, J = 8 Hz, 1H), 8.69 (s, 1H); ESI-HRMS: $[M-H]^-$ calcd for $C_{22}H_{27}N_5O_3S$: 440.1756, found: 440.1746.

4.2.6. 1-(1-Adamantyl)-3-(4-(*N*-(3,4-dimethylisoxazol-5-yl) benzenesulfonamide))urea (12)

21 mg (4.7%) as a brown oil; ^{1}H NMR (DMSO-d_6) δ = 1.62 (s, 3H), 1.64 (br, 6H), 1.94 (br, 6H), 2.04 (br, 3H), 2.07 (s, 3H), 6.07 (s, 1H), 7.51 (d, J = 8 Hz, 2H), 7.58 (d, J = 8 Hz, 2H), 8.76 (s, 1H), 10.79 (s, 1H); ESI-HRMS: $[M-H]^-$ calcd for $C_{22}H_{27}N_4O_4S$: 443.1753, found: 443.1747.

4.2.7. 1-(1-Adamantyl)-3-(4-((4-aminophenyl) sulfonyl)phenyl)urea (13)

12 mg (2.8%) as white solid; MP = 254–256 °C; ^{1}H NMR (DMSO-d_6) δ = 1.62 (br, 6H), 1.92 (br, 6H), 2.02 (br, 3H), 6.02 (s, 1H), 6.08 (s, 2H), 6.60 (d, J = 8 Hz, 2H), 7.46 (d, J = 8 Hz, 2H), 7.49 (d, J = 8 Hz, 2H), 7.65 (d, J = 8 Hz, 2H), 8.71 (s, 1H); ^{13}C NMR (DMSO-d_6) δ = 28.82, 35.94, 41.42, 50.03, 112.86, 116.86, 126.60, 127.75, 128.93, 134.29, 144.47, 153.16; ESI-HRMS: $[M+H]^+$ calcd for $C_{23}H_{26}N_3O_3S$: 426.1851, found: 426.1834.

4.3. General methods for 1-(1-adamantyl)-3-(heteraryl)ureas

4.3.1. Method A

1-Adamantyl isocyanate (177 mg, 1.0 mmol), heteroarylamine (1.2 mmol) and triethylamine (502 μL, 3.6 mmol) were dissolved in THF (1.5 mL) and stirred for 72 h at 70 °C. The solvent was removed under reduced pressure and the residue was purified by normal phase flash column chromatography using a hexane to ethyl acetate gradient.

4.3.2. Method B

Heteroarylamine (1.0 mmol) was added to THF (20 mL) and cooled on a dry ice in acetone bath. To that, butyllithium (400 μL, 1.0 mmol, 2.5 M in hexane) was added dropwise over 20 min. The reaction mixture was removed from the dry ice in acetone bath and 1-adamantyl isocyanate (177 mg, 1.0 mmol) was added and stirred for 1 h. Methanol (4 mL) was then added to quench any unreacted butyllithium. The solvents were then removed under reduced pressure and the residue was purified by normal phase flash column chromatography using a hexane to ethyl acetate gradient.

4.3.3. 1-(1-Adamantyl)-3-(4-pyridinyl)urea (14)

Method A; 34 mg (12.4%) of white powder; MP = 200–202 °C; ^{1}H NMR ($CDCl_3$) δ = 1.70 (br, 6H), 2.01 (br, 6H), 2.10 (br, 3H), 7.35 (d, J = 8 Hz, 2H), 8.22 (d, J = 8 Hz, 2H); ESI-HRMS: $[M+H]^+$ calcd for $C_{16}H_{22}N_3O$: 272.1763, found: 272.1767.

4.3.4. 1-(1-Adamantyl)-3-(3-pyridinyl)urea (15)

Method B; 58 mg (21.4%) of tan powder; MP = 202–204 °C; ^{1}H NMR (DMSO-d_6) δ = 1.64 (br, 6H), 1.94 (br, 6H), 2.04 (br, 3H), 6.00 (s, 1H), 7.23 (dd, J = 8 Hz, 1H), 7.85 (d, J = 8 Hz, 1H), 8.09 (d, 1H), 8.42 (s, 1H), 8.45 (s, 1H); ESI-HRMS: $[M+H]^+$ calcd for $C_{16}H_{22}N_3O$: 272.1763, found: 272.1767.

4.3.5. 1-(1-Adamantyl)-3-(2-pyridinyl)urea (16)

Method B; 78 mg (28.7%) of white powder; MP = 205–206 °C; ^{1}H NMR (DMSO-d_6) δ = 1.65 (br, 6H), 1.98 (br, 6H), 2.04 (br, 3H), 6.88 (dd, J = 8 Hz, 1H), 7.32 (d, J = 8 Hz, 1H), 7.64 (t, J = 8 Hz, 1H), 8.09 (s, 1H), 8.14 (d, J = 8 Hz, 1H), 8.94 (s, 1H); ESI-HRMS: $[M+H]^+$ calcd for $C_{16}H_{22}N_3O$: 272.1763, found: 272.1767.

4.3.6. 1-(1-Adamantyl)-3-(2-pyrimidinyl)urea (17)

Method B; 183 mg (67.2%) of white powder; MP = 267–270 °C; ^{1}H NMR ($CDCl_3$) δ = 1.54 (br, 9H), 2.10 (br, 6H), 6.85 (t, J = 8 Hz, 1H), 7.17 (s, 1H), 8.45 (d, J = 8 Hz, 2H), 8.86 (s, 1H); ESI-HRMS: $[M+H]^+$ calcd for $C_{15}H_{21}N_4O$: 273.1715, found: 273.1745.

4.3.7. 1-(1-Adamantyl)-3-(4-pyrimidinyl)urea (18)

Method B; 126 mg (46.3%) of white powder; MP = 199–201 °C; ^{1}H NMR (DMSO-d_6) δ = 1.64 (br, 6H), 1.96 (br, 6H), 2.04 (br, 3H), 7.50 (s, 1H), 7.54 (d, J = 8 Hz, 1H), 8.43 (d, J = 8 Hz, 1H), 8.68 (s, 1H), 9.39 (s, 1H); ESI-HRMS: $[M+H]^+$ calcd for $C_{15}H_{21}N_4O$: 273.1715, found: 273.1711.

4.3.8. 1-(1-Adamantyl)-3-(4-(1,3,5-triazolyl))urea (19)

Method B; 28 mg (10.2%) of tan powder; MP = 231–233 °C; ^{1}H NMR ($CDCl_3$) δ = 1.72 (br, 6H), 2.09 (br, 9H), 8.58 (s, 1H), 8.82 (s, 1H); ESI-HRMS: $[M+H]^+$ calcd for $C_{14}H_{20}N_5O$: 274.1668, found: 274.1674.

4.3.9. 1-(1-Adamantyl)-3-(3-(1,2,4-triazolyl))urea (20)

Method B; 63 mg (23.1%) of tan powder; MP = 201–204 °C; ^{1}H NMR ($CDCl_3$) δ = 1.72 (br, 6H), 2.11 (br, 9H), 7.61 (s, 1H), 8.40 (s, 1H), 8.63 (s, 1H), 8.85 (s, 1H); ESI-HRMS: $[M+H]^+$ calcd for $C_{14}H_{20}N_5O$: 274.1668, found: 274.1674.

4.3.10. 1-(1-Adamantyl)-3-(2-oxazolyl)urea (21)

Method B; 112 mg (42.9%) of white powder; MP = 178–182 °C; ^{1}H NMR (DMSO-d_6) δ = 1.64 (br, 6H), 1.97 (br, 6H), 2.04 (br, 3H), 7.02 (s, 1H), 7.71 (s, 1H), 8.14 (s, 1H), 10.31 (s, 1H); ^{13}C NMR (DMSO-d_6) δ = 28.81, 35.89, 41.31, 50.32, 125.51, 133.91, 150.53, 155.72; ESI-HRMS: $[M+H]^+$ calcd for $C_{14}H_{20}N_3O_2$: 262.1556, found: 262.1562.

4.3.11. 1-(1-Adamantyl)-3-(3-isoxazolyl)urea (22)

Method B; 66 mg (25.3%) of white powder; MP = 166–167 °C; ^{1}H NMR ($CDCl_3$) δ = 1.72 (br, 6H), 2.10 (br, 9H), 6.36 (s, 1H), 7.29 (s, 1H), 8.18 (s, 1H), 9.41 (s, 1H); ESI-HRMS: $[M+H]^+$ calcd for $C_{14}H_{20}N_3O_2$: 262.1556, found: 262.1550.

4.3.12. 1-(1-Adamantyl)-3-(5-methylisoxazol-3-yl)urea (23)

Method B; 218 mg (79.0%) of tan powder; MP = 179–180 °C; ^{1}H NMR (DMSO-d_6) δ = 1.63 (br, 6H), 1.92 (br, 6H), 2.03 (br, 3H), 2.31 (s, 3H), 6.31 (s, 1H), 6.36 (s, 1H), 8.96 (s, 1H); ESI-HRMS: $[M+H]^+$ calcd for $C_{15}H_{22}N_3O_2$: 276.1712, found: 276.1721.

4.3.13. 1-(1-Adamantyl)-3-(5-*t*-butylisoxazol-3-yl)urea (24)

Method B; 48 mg (15.12%) of white powder; MP = 195–196 °C; ^{1}H NMR ($CDCl_3$) δ = 1.32 (s, 9H), 1.70 (br, 6H), 2.08 (br, 9H), 6.01 (s, 1H), 6.75 (s, 1H), 9.38 (s, 1H); ^{13}C NMR ($CDCl_3$) δ = 28.58, 29.53, 32.76, 36.44, 41.95, 51.56, 91.90, 153.91, 159.24, 180.42; ESI-HRMS: $[M+H]^+$ calcd for $C_{18}H_{28}N_3O_2$: 318.2182, found: 318.2171.

4.3.14. 1-(1-Adamantyl)-3-(4-bromo-5-methylisoxazol-3-yl)urea (25)

Method B; 92 mg (26.0%) of white powder; MP = 193–197 °C; ^{1}H NMR ($CDCl_3$) δ = 1.64 (br, 6H), 2.01 (br, 6H), 2.04 (br, 3H), 2.31 (s, 3H), 6.23 (s, 1H), 7.14 (s, 1H); ESI-HRMS: $[M+H]^+$ calcd for $C_{15}H_{22}BrN_3O_2$: 354.0817, found: 354.0812.

4.3.15. 1-(1-Adamantyl)-3-((5-methylisoxazol-3-yl)methyl)urea (26)

Method A; 101 mg (34.9%) of white powder; MP = 207–209 °C; ^{1}H NMR (DMSO-d_6) δ = 1.61 (br, 6H), 1.87 (br, 6H), 2.00 (br, 3H), 2.37 (s, 3H), 4.13 (d, J = 8 Hz, 2H), 5.70 (s, 1H), 6.05 (s, 1H), 6.11 (t, J = 8 Hz, 1H); ESI-HRMS: $[M+H]^+$ calcd for $C_{16}H_{24}N_3O_2$: 290.1869, found: 290.1865.

4.3.16. 1-(1-Adamantyl)-3-(3-methylisoxazol-5-yl)urea (27)

Method B; 125 mg (45.4%) of white powder; MP = 183–187 °C; ^{1}H NMR ($CDCl_3$) δ = 1.65 (br, 6H), 1.97 (br, 6H), 2.05 (br, 3H), 2.23 (s, 3H), 5.82 (s, 1H), 5.92 (s, 1H), 8.84 (s, 1H); ESI-HRMS: $[M+H]^+$ calcd for $C_{15}H_{22}N_3O_2$: 276.1712, found: 276.1721.

4.3.17. 1-(1-Adamantyl)-3-(3-trifluoromethylisoxazol-5-yl)urea (28)

Method B; 75 mg (22.8%) of white powder; MP = 264–268 °C; ^{1}H NMR ($CDCl_3$) δ = 1.63 (br, 6H), 1.94 (br, 6H), 2.05 (br, 3H), 4.76 (s, 1H), 6.29 (s, 1H), 7.45 (s, 1H); ^{13}C NMR (DMSO-d_6) δ = 28.78, 35.79, 41.12, 50.49, 81.67, 119.67 (q, J = 1076 Hz), 149.83, 155.10 (q, J = 148 Hz), 164.40; ESI-HRMS: $[M+H]^+$ calcd for $C_{15}H_{19}F_3N_3O_2$: 330.1429, found: 330.1476.

4.3.18. 1-(1-Adamantyl)-3-(4-chloro-3-methylisoxazol-5-yl)urea (29)

Method B; 29 mg (9.4%) of white powder; MP = 178–183 °C; ^{1}H NMR ($CDCl_3$) δ = 1.63 (br, 6H), 1.97 (br, 6H), 2.04 (br, 3H), 2.17 (s, 3H), 5.80 (s, 1H); ESI-HRMS: $[M+H]^+$ calcd for $C_{15}H_{21}ClN_3O_2$: 310.1322, found: 310.1317.

4.3.19. 1-(1-Adamantyl)-3-(4-cyano-3-methylisoxazol-5-yl)urea (30)

Method B; 57 mg (19.0%) of white powder; MP = 191–196 °C; ^{1}H NMR ($CDCl_3$) δ = 1.70 (br, 6H), 2.05 (br, 6H), 2.12 (br, 3H), 2.34 (s, 3H), 5.72 (s, 1H), 8.41 (s, 1H); ESI-HRMS: $[M+H]^+$ calcd for $C_{16}H_{21}N_4O_2$: 301.1665, found: 301.1677.

4.3.20. 1-(1-Adamantyl)-3-(3,4-dimethylisoxazol-5-yl)urea (31)

Method B; 12 mg (4.2%) of grey wax; ^{1}H NMR ($CDCl_3$) δ = 1.68 (br, 6H), 1.87 (s, 3H), 2.02 (br, 6H), 2.09 (br, 3H), 2.18 (s, 3H), 5.69 (s, 1H), 7.40 (s, 1H); ESI-HRMS: $[M+H]^+$ calcd for $C_{16}H_{24}N_3O_2$: 290.1869, found: 290.1865.

4.3.21. 1-(1-Adamantyl)-3-(thiazol-2-yl)urea (32)

Method A; 156 mg (56.2%) of white powder; MP = 173–174 °C; ^{1}H NMR (DMSO-d_6) δ = 1.64 (br, 6H), 1.93 (br, 6H), 2.04 (br, 3H), 6.33 (s, 1H), 6.99 (d, J = 4 Hz, 1H), 7.27 (d, J = 4 Hz, 1H), 10.01 (s, 1H); ^{13}C NMR (DMSO-d_6) δ = 28.83, 35.87, 41.40, 50.23, 111.54, 137.20, 152.31, 159.74; ESI-HRMS: $[M+H]^+$ calcd for $C_{14}H_{20}N_3OS$: 278.1327, found: 278.1329.

4.3.22. 1-(1-Adamantyl)-3-(4-methylthiazol-2-yl)urea (33)

Method A; 155 mg (53.2%) of white powder; MP = 223–224 °C; ^{1}H NMR (DMSO-d_6) δ = 1.64 (br, 6H), 1.92 (br, 6H), 2.04 (br, 3H), 2.17 (s, 3H), 6.35 (s, 1H), 6.52 (s, 1H), 9.90 (s, 1H); ^{13}C NMR (DMSO-d_6) δ = 16.96, 28.83, 35.87, 41.40, 50.22, 105.69, 146.10, 152.31, 159.09; ESI-HRMS: $[M+H]^+$ calcd for $C_{15}H_{22}N_3OS$: 292.1484, found: 292.1473.

4.3.23. 1-(1-Adamantyl)-3-(5-methylthiazol-2-yl)urea (34)

Method A; 138 mg (47.4%) of white powder; MP = 233–235 °C; ^{1}H NMR (DMSO-d_6) δ = 1.64 (br, 6H), 1.92 (br, 6H), 2.04 (br, 3H), 2.27 (s, 3H), 6.32 (s, 1H), 6.93 (s, 1H), 9.80 (s, 1H); ^{13}C NMR (DMSO-d_6) δ = 11.12, 28.82, 35.88, 41.42, 50.18, 99.51, 124.08, 134.17, 152.26, 158.05; ESI-HRMS: $[M+H]^+$ calcd for $C_{15}H_{22}N_3OS$: 292.1484, found: 292.1473.

4.3.24. 1-(1-Adamantyl)-3-(benzothiazol-2-yl)urea (35)

Method A; 30 mg (9.16%) of white powder; Decomposes; ^{1}H NMR (DMSO-d_6) δ = 1.66 (br, 6H), 1.97 (br, 6H), 2.06 (br, 3H), 6.57 (s, 1H), 7.20 (t, J = 8 Hz, 1H), 7.37 (t, J = 8 Hz, 1H), 7.60 (d, J = 8 Hz, 1H), 7.86 (d, J = 8 Hz, 1H), 10.24 (s, 1H); ^{13}C NMR ($CDCl_3$) δ = 29.52, 36.38, 41.94, 51.87, 120.03, 121.25, 123.30, 126.06, 130.79, 149.30, 153.08, 161.81; ESI-HRMS: $[M+H]^+$ calcd for $C_{18}H_{22}N_3OS$: 328.1484, found: 328.1483.

4.3.25. 1-(1-Adamantyl)-3-(5-methyl-1,3,4-oxadiazol-2-yl)urea (36)

Method B; 84 mg (30.4%) of white powder; MP = 173–176 °C; ^{1}H NMR (DMSO-d_6) δ = 1.64 (br, 6H), 1.96 (br, 6H), 2.05 (br, 3H), 2.38 (s, 3H), 7.46 (s, 1H), 10.46 (s, 1H); ESI-HRMS: $[M+H]^+$ calcd for $C_{14}H_{21}N_4O_2$: 277.1665, found: 277.1670.

4.3.26. 1-(1-Adamantyl)-3-(5-isopropyl-1,3,4-oxadiazol-2-yl)urea (37)

Method B; 76 mg (25.0%) of white powder; MP = 164–165 °C; ^{1}H NMR (DMSO-d_6) δ = 1.25 (d, J = 8 Hz, 6H), 1.64 (br, 6H), 1.96 (br, 6H), 2.05 (br, 3H), 3.08 (sep, 1H), 7.47 (s, 1H), 10.44 (s, 1H); ^{13}C NMR (DMSO-d_6) δ = 19.52, 25.34, 28.80, 35.85, 41.18, 50.59, 150.06, 158.74, 165.33; ESI-HRMS: $[M+H]^+$ calcd for $C_{16}H_{25}N_4O_2$: 305.1978, found: 305.1986.

4.3.27. 1-(1-Adamantyl)-3-(5-cyclopropyl-1,3,4-oxadiazol-2-yl)urea (38)

Method B; 53 mg (17.5%) of white powder; MP = 161–165 °C; ^{1}H NMR (DMSO-d_6) δ = 0.88–0.92 (m, 2H), 1.03–1.08 (m, 2H), 1.64 (br, 6H), 1.95 (br, 6H), 2.04 (br, 3H), 2.09 (sep, 1H), 7.41 (s, 1H), 10.39 (s, 1H); ESI-HRMS: $[M+H]^+$ calcd for $C_{16}H_{23}N_4O_2$: 303.1821, found: 303.1837.

4.3.28. 1-(1-Adamantyl)-3-(5-cyclobutyl-1,3,4-oxadiazol-2-yl) urea (39)

Method A; 173 mg (54.7%) of white powder; MP = 161–163 °C; ^{1}H NMR (DMSO-d_6) δ = 1.64 (br, 6H), 1.85–1.98 (m, 7H), 2.00–2.09 (m, 4H), 2.20–2.38 (m, 4H), 3.64 (pen, 1H), 7.47 (s, 1H), 10.45 (s, 1H); ESI-HRMS: $[M+H]^+$ calcd for $C_{17}H_{25}N_4O_2$: 317.1978, found: 317.1985.

4.3.29. 1-(1-Adamantyl)-3-(5-(thiophen-2-yl)-1,3,4-oxadiazol-2-yl)urea (40)

Method A; 146 mg (42.4%) of white powder; MP = 211–213 °C; ^{1}H NMR (DMSO-d_6) δ = 1.65 (br, 6H), 1.98 (br, 6H), 2.06 (br, 3H), 7.26 (t, J = 4 Hz, 1H), 7.36 (s, 1H), 7.63 (d, J = 4 Hz, 1H), 7.88 (d, J = 4 Hz, 1H), 10.66 (s, 1H); ESI-HRMS: $[M+H]^+$ calcd for $C_{17}H_{21}N_4O_2S$: 345.1385, found: 345.1383.

4.3.30. 1-(1-Adamantyl)-3-(1-ethylpyrazol-3-yl)urea (41)

Method A; 162 mg (56.2%) of white powder; MP = 140–146 °C; ^{1}H NMR (DMSO-d_6) δ = 1.31 (t, J = 8 Hz, 3H), 1.63 (br, 6H), 1.93 (br, 6H), 2.03 (br, 3H), 3.95 (q, J = 8 Hz, 2H), 5.97 (s, 1H), 7.49 (s, 1H), 8.47 (s, 1H); ESI-HRMS: $[M+H]^+$ calcd for $C_{16}H_{25}N_4O$: 289.2028, found: 289.2033.

4.3.31. 1-(1-Adamantyl)-3-(1-ethyl-5-methylpyrazol-3-yl)urea (42)

Method A; 158 mg (52.2%) of white powder; MP = 215–217 °C; ^{1}H NMR (DMSO-d_6) δ = 1.24 (t, J = 8 Hz, 3H), 1.63 (br, 6H), 1.93 (br, 6H), 2.02 (br, 3H), 2.16 (s, 3H), 3.86 (q, J = 8 Hz, 2H), 5.75 (s, 1H), 6.91 (s, 1H), 8.37 (s, 1H); ESI-HRMS: $[M+H]^+$ calcd for $C_{17}H_{27}N_4O$: 303.2185, found: 303.2193.

4.3.32. 1-(1-Adamantyl)-3-(5-methyl-1-propylpyrazol-3-yl)urea (43)

Method A; 160 mg (50.6%) of white powder; MP = 200–201 °C; ^{1}H NMR (DMSO-d_6) δ = 0.82 (t, J = 8 Hz, 3H), 1.63 (br, 6H), 1.68 (sex, J = 8 Hz, 2H), 1.92 (br, 6H), 2.02 (br, 3H), 2.16 (s, 3H), 3.78 (q, J = 8 Hz, 2H), 5.75 (s, 1H), 6.87 (s, 1H), 8.38 (s, 1H); ^{13}C NMR (DMSO-d_6) δ = 10.59, 10.99, 22.82, 28.88, 36.04, 41.73, 48.95, 49.66, 99.51, 138.25, 147.47, 153.32; ESI-HRMS: $[M+H]^+$ calcd for $C_{18}H_{29}N_4O$: 317.2341, found: 317.2349.

4.3.33. 1-(1-Adamantyl)-3-(1-methylpyrazol-4-yl)urea (44)

Method A; 174 mg (63.4%) of white powder; MP = 217–218 °C; ^{1}H NMR (DMSO-d_6) δ = 1.62 (br, 6H), 1.90 (br, 6H), 2.01 (br, 3H), 3.73 (s, 3H), 5.68 (s, 1H), 7.21 (s, 1H), 7.60 (s, 1H), 7.84 (s, 1H); ESI-HRMS: $[M+H]^+$ calcd for $C_{15}H_{23}N_4O$: 275.1872, found: 275.1858.

4.4. General procedure for 1-(2-adamantyl)-3-(heteroaryl)urea

Triphosgene (119 mg, 0.4 mmol) was dissolved in DCM (10 mL) and cooled on an acetone and dry ice bath. A solution of heteroarylamine (1 mmol) and DIPEA (393 μL, 2.2 mmol) in THF (5 mL) was then added dropwise over 15 min. After the reaction mixture stirred for an additional 5 min, a suspension of 2-adamantylamine hydrogen chloride (188 mg, 1.0 mmol) and DIPEA (393 μL, 2.2 mmol) in DCM (5 mL) was added. The reaction mixture was removed from the acetone and dry ice bath and stirred for 1 h. The solvents were removed under reduced pressure and the crude residue was purified by normal phase flash column chromatography using a hexane to ethyl acetate gradient.

4.4.1. 1-(2-Adamantyl)-3-(oxazol-2yl)urea (45)

53 mg (40.6%) of white powder; MP = 189–192 °C; ^{1}H NMR ($CDCl_3$) δ = 1.65 (1H, s), 1.68 (1H, s), 1.78 (2H, s), 1.89 (6H, br), 1.97–2.00 (m, 4H), 4.09 (1H, d, J = 8 Hz), 8.62 (1H, d, J = 8 Hz), 9.77 (1H, s); ESI-HRMS: $[M+H]^+$ calcd for $C_{14}H_{20}N_3O_2$: 262.1550, found: 262.1583.

4.4.2. 1-(2-Adamantyl)-3-(5-*t*-butylisoxazol-3-yl)urea (46)

167 mg (48.7%) of white powder; MP = 229–232 °C; ^{1}H NMR (DMSO-d_6) δ = 1.27 (s, 9H), 1.56 (s, 1H), 1.59 (s, 1H), 1.65–1.88 (m, 12H), 3.78 (d, J = 8 Hz, 1H), 6.28 (s, 1H), 6.98 (d, J = 8 Hz, 1H), 9.26 (s, 1H); ^{13}C NMR ($CDCl_3$) δ = 27.18, 27.32, 28.63, 31.96, 32.38, 37.19, 37.63, 54.45, 91.93, 154.55, 159.14, 180.50; ESI-HRMS: $[M+H]^+$ calcd for $C_{18}H_{28}N_3O_2$: 318.2182, found: 318.2171.

4.4.3. 1-(2-Adamantyl)-3-(5-methylisoxazol-3-yl)urea (47)

64 mg (24.5%) of white powder; MP = 208–212 °C; ^{1}H NMR (DMSO-d_6) δ = 1.32 (s, 1H), 1.35 (s, 1H), 1.44–1.63 (m, 12H), 3.54 (d, J = 8 Hz, 1H), 6.10 (s, 1H), 6.72 (d, J = 8 Hz, 1H), 8.95 (s, 1H); ^{13}C NMR ($CDCl_3$) δ = 11.97, 26.54, 26.64, 31.18, 31.87, 36.62, 37.02, 53.06, 95.14, 152.81, 159.12, 168.69; ESI-HRMS: $[M+H]^+$ calcd for $C_{15}H_{22}N_3O_2$: 276.1712, found: 276.1721.

4.4.4. 1-(2-Adamantyl)-3-(4-methylthiazol-2-yl)urea (48)

14 mg (9.6%) of off white powder; MP = 229–231 °C; ^{1}H NMR ($CDCl_3$) δ = 1.50 (1H, s), 1.53 (1H, s), 1.61 (2H, s), 1.67–1.74 (7H, br), 1.78 (1H, s), 1.83 (2H, s), 3.88 (1H, d, J = 8 Hz), 6.17 (1H, s); ^{13}C NMR ($CDCl_3$) δ = 17.38, 27.15, 27.44, 31.97, 32.43, 37.17, 37.64, 54.19, 104.85, 147.22, 154.22, 161.89; ESI-HRMS: $[M+H]^+$ calcd for $C_{15}H_{22}N_3O_2$: 292.1478, found: 292.1473.

4.4.5. 1-(2-Adamantyl)-3-(5-isopropyl-1,3,4-oxadiazol-2-yl)urea (49)

96 mg (63.1%) of white powder; MP = 172–174 °C; ^{1}H NMR (DMSO-d_6) δ = 1.02 (6H, d, J = 8.0 Hz), 1.36 (1H, s), 1.39 (1H, s), 1.48 (2H, s), 1.51 (1H, s), 1.55 (2H, s), 1.58–1.61 (7H, m), 2.85 (1H, sep, J = 8 Hz), 3.62 (1H, d, J = 8 Hz), 7.97 (1H, d, J = 8 Hz), 10.23 (1H, s); ^{13}C NMR ($CDCl_3$) δ = 19.76, 26.19, 27.12, 27.22, 31.88, 32.24, 37.10, 37.56, 54.71, 152.39, 158.75, 166.06; ESI-HRMS: $[M+H]^+$ calcd for $C_{16}H_{25}N_4O_2$: 305.1972, found: 305.1957.

4.4.6. 1-(2-Adamantyl)-3-(5-cyclopropyl-1,3,4-oxadiazol-2-yl) urea (50)

13 mg (8.6%) of white powder; MP = 179–181 °C; ^{1}H NMR ($CDCl_3$) δ = 1.12–1.14 (4H, m), 1.65 (1H, s), 1.68 (1H, s), 1.78 (2H, s), 1.89 (6H, br), 1.96 (1H, s), 2.00 (3H, br), 2.03–2.09 (1H, m), 4.08 (1H, d, J = 8 Hz), 8.56 (1H, d, J = 8 Hz), 8.65 (1H, s); ^{13}C NMR ($CDCl_3$) δ = 5.95, 7.93, 27.12, 27.22, 31.89, 32.23, 37.10, 37.57, 54.76, 151.58, 157.89, 163.57; ESI-HRMS: $[M+H]^+$ calcd for $C_{17}H_{27}N_4O$: 303.1816, found: 303.1809.

4.4.7. 1-(2-Adamantyl)-3-(5-cyclobutyl-1,3,4-oxadiazol-2-yl)urea (51)

84 mg (53.1%) of white powder; MP = 193–196 °C; ^{1}H NMR (DMSO-d_6) δ = 1.61 (1H, s), 1.63 (1H, s), 1.73 (2H, s), 1.76–1.79 (2H, m), 1.83–1.85 (8H, m), 1.89–1.97 (1H, m), 1.99–2.10 (1H, s), 2.23–2.38 (4H, m), 3.65 (1H, pen, J = 8 Hz), 3.87 (1H, d, J = 8 Hz), 8.21 (1H, d, J = 8 Hz), 10.77 (1H, s); ^{13}C NMR ($CDCl_3$) δ = 18.82, 26.78, 27.13, 27.23, 30.22, 31.89, 32.25, 37.11, 37.58, 54.73, 152.28, 158.67, 164.41; ESI-HRMS: $[M+H]^+$ calcd for $C_{17}H_{25}N_4O_2$: 317.1972, found: 317.2020.

4.4.8. 1-(2-Adamantyl)-3-(1-ethyl-5-methylpyrazol-3-yl)urea (52)

14 mg (9.26%) of white powder; MP = 159–163 °C; ^{1}H NMR ($CDCl_3$) δ = 1.32 (3H, t, J = 8.0 Hz), 1.57 (1H, s), 1.60 (1H, s), 1.69 (2H, s), 1.80 (6H, br), 1.90 (4H, br), 2.14 (3H, s), 3.87 (2H, q, J = 8 Hz), 3.98 (1H, d, J = 8 Hz), 5.40 (1H, s), 6.55 (1H, s), 8.48 (1H,

s); ^{13}C NMR (DMSO-d_6) δ = 10.40, 14.89, 26.60, 26.80, 31.36, 32.13, 36.71, 37.13, 42.50, 52.79, 93.71, 138.09, 147.58, 153.80; ESI-HRMS: $[M+H]^+$ calcd for $C_{17}H_{27}N_4O$: 303.2179, found: 303.2170.

4.4.9. 1-(2-Adamantyl)-3-(5-methyl-1-propylpyrazol-3-yl)urea (53)

82 mg (51.8%) of white powder; MP = 206–209 °C; ^{1}H NMR ($CDCl_3$) δ = 0.93 (3H, t, J = 8.0 Hz), 1.65 (1H, s), 1.68 (1H, s), 1.78 (2H, s), 1.80–1.92 (8H, m), 1.99 (4H, br), 3.88 (2H, t, J = 8 Hz), 4.07 (1H, d, J = 8 Hz), 5.48 (1H, s), 6.49 (1H, s), 8.62 (1H, d, J = 8 Hz); ^{13}C NMR (DMSO-d_6) δ = 11.00, 11.21, 23.23, 27.26, 27.58, 32.13, 32.58, 37.20, 37.81, 50.08, 53.99, 93.10, 139.11, 147.64, 154.53; ESI-HRMS: $[M+H]^+$ calcd for $C_{18}H_{29}N_4O$: 317.2336, found: 317.2320.

4.5. MIC determination

MIC values were determined against *M. tb* using microbroth dilution method in accordance with the CLSI and to our previously published methods.[9,13] Compounds were initially dissolved in DMSO at 10 mg/mL and stored at −80 °C until needed. Compounds stocks were diluted in Middlebrook 7H9 media (final volume of 100 μL) and serially diluted in a 96-well round bottom microtitre plate. *M. tb* culture was grown in Middlebrook 7H9 media with 0.05% Tween 80 at 37 °C to an OD_{600} of 0.003 providing approximately 10^5 cfu/mL. *M. tb* culture (100 μL) was then added to the drug plates giving 200 μL total volume and final drug concentrations beginning at 200 μg/mL. The plates were incubated at 37 °C for seven days and visual inspection was used to determine the minimum concentration of drug that inhibited >90% of bacterial growth.

4.6. Human soluble epoxide hydrolase assay

The IC_{50} values were determined using previously published methods.[14] The fluorescent substrate used was cyano(2-methoxynaphthalen-6-yl)methyl trans-(3-pheyloxyran-2-yl)methyl carbonate (CMNPC). Inhibitor and purified recombinant human sEH[15,16] (1 nM) were incubated together for 5 min in pH 7.4 sodium phosphate buffer (100 mM) which contained BSA (0.1 mg/mL) at 30 °C. CMNPC addition subsequently followed (final CMNPC concentration = 5 μM). Enzyme activity was determined by monitoring the appearance of 6-methoxy-2-naphthaldehyde over 10 min by fluorescence detection with excitation and emission wavelengths of 330 and 465 nm, respectively. The IC_{50} values reported are the average of three replicates with at least two data points above and below the IC_{50}. The assay as performed here has a standard error between 10% and 20%, suggesting that differences of twofold or greater are significant.[14]

4.7. Cytotoxicity determination

Vero epithelial cells (ATCC CCL-81) were grown in Dulbecco's modified Eagle's medium (DMEM) supplemented with 10% fetal bovine serum (FBS) at 37 °C in a humidified incubator with 5% CO_2. Trypsinized cells were transferred to 96-well cell culture plates (Nunc) at a seeding density of $\sim 5 \times 10^3$ cells per well. The next day, when cells were ~10% confluent, DMEM/FBS was exchanged for fresh media containing twofold serial dilutions of test compounds and cells were incubated for an additional 72 h. MTT cell proliferation assay was performed as described by manufacturer (Promega Corporation, Madison, WI) with absorbances read following overnight solubilization of formazan. IC_{50} values were derived from corresponding dose–response curves.

4.8. Solubility determination

Compounds were initially prepared by dissolving them into DMSO at a final concentration of 10 mM. Stock drug plates were prepared by adding 30 μL of 10 mM DMSO stocks to each well in a 96-well plate. For reference plates, compounds were diluted 600-fold in system solution buffer (SSB, pH 7.4; pION INC, Woburn, MA) and *iso*-propanol (1:1, v/v). Concentrations were assessed by UV spectrometry (230–500 nm). For sample plates, compounds were diluted 100-fold in system solution buffer, incubated at room temperature for 18 h to allow the compounds to be fully stable, and then filtered through a 96-well filter plate (pION Inc., Woburn, MA). Fractions were collected from the filtered sample plate, diluted with *iso*-propanol by 1:1 (v/v), and determined concentration via UV spectrometry. Calculation was carried out by μSOL Evolution software and all compounds were tested in triplicates.

4.9. Human plasma protein binding determination

Compounds were initially prepared by dissolving them into DMSO at a final concentration of 10 mM. Dulbecco's phosphate buffered saline (DPBS; pH 7.4) was obtained from Invitrogen (Carlsbad, CA), single-use RED (rapid equilibrium dialysis) device was obtained from Thermo scientific (Rockford, IL) and human plasma was obtained from Innovative Research INC (Novi, Michigan, IL).

Sample preparation for plasma protein binding was modified from Waters' method.[17] Teflon base plates with the RED inserts (molecular weight cut-off (MWCO) = 8000) were to used without any pre-conditioning of the membrane inserts. Human plasma was thawed and centrifuged at 1000 rpm for 2 min to remove any particulates. Each compound was prepared at 10 μM in human plasma. These samples were prepared by adding 1 μL of drug stock to 1000 μL of human plasma. Spiked plasma solutions (300 μL) were placed into the sample chamber (indicated by the red ring) and 500 μL of DPBS into the adjacent chamber. The plate was sealed and incubated at 37 °C on an orbital shaker (100 rpm) for 4 h. After incubation, the seal was removed from the RED plate and the volume of the insert was inspected to ensure minimal volume change. Aliquots (50 μL) were removed from each side of the insert and dispensed into a 96-well deep plate. An equal volume of blank plasma or DPBS was added to the required wells to create analytically identical sample matrices. To each sample, 200 μL of ACN containing the internal standard (4 μg/mL warfarin) was added. All of the plates were sealed and mixed well at 600 rpm for 10 min and were centrifuged at 4000 rpm for 20 min. The supernatants (120 μL) were transferred to analytical plates for analysis by LCMS. LCMS conditions were described in the materials and instrumentation section above. The test compound concentrations were quantified in both buffer and plasma chambers via peak areas relative to the internal standard. The percentage of the test compound bound to plasma was calculated on following equations:

$$\%\text{Free} = \frac{[\text{Buffer Chamber}]}{[\text{Plasma Chamber}]} \times 100 \quad (1)$$

%Bound = 100 − %Free.

4.10. Microsomal stability determination

Compounds were initially prepared by dissolving them into DMSO at a final concentration of 10 mM. NADPH regenerating solutions A and B and mouse liver microsomes (CD-1) were obtained from BD Gentest (Woburn, MA). Ninety-six deep well plates were obtained from MidWest Scientific Inc. (Valley Park, MO).

Sample preparation for microsomal stability was modified from Di's methods.[18,19] A set of incubation times of 0, 15, 30, 60, 120, and 240 min were used. Human or mouse liver microsomal solutions were prepared by adding 58 μL of concentrated human or mouse liver microsomes (20 mg/mL protein concentration) to 1.756 mL of 0.1 M potassium phosphate buffer (pH 7.4) and 5 μL of 0.5 M EDTA to make a 0.6381 mg/mL (protein) microsomal solution. NADPH regenerating agent contained 113 μL of NADPH A, 23 μL of NADPH B, and 315 μL of 0.1 M potassium phosphate buffer (pH 7.4). The diluted test compound solutions (2 μL) were each added directly to a 1.79 mL of liver microsomal solution. This solution was mixed and 90 μL was transferred to six time points plates (each in triplicate wells). For the time 0 plate, 225 μL of cold acetonitrile with internal standard (4 mg/ml warfarin) was added to each well, followed by addition of NADPH regenerating agent (22.5 μL) and no incubation. For other five time points' plate, NADPH regenerating agent (22.5 μL) was added to each well to initiate the reaction. The plates were incubated at 37 °C for the required time, followed by quenching of the reaction by adding 225 μL of cold acetonitrile with internal standard (4 μg/ml warfarin). All of the plates were sealed and mixed well at 600 rpm for 10 min followed by centrifugation at 4000 rpm for 20 min. The supernatants (120 μL) were transferred to analytical plates for analysis by LCMS. LCMS conditions were described in the materials and instrumentation section above. The metabolic stability is evaluated via the half-life from least-squares fit of the multiple time points based on first-order kinetics.

4.11. Permeability determination

Compounds were initially prepared by dissolving them into DMSO at a final concentration of 10 mM. Drug stock plates were prepared by adding 6 μL of DMSO solutions to each well. Compounds were diluted 200-fold in system solution buffer (SSB, pH 7.4; pION INC, Woburn, MA). The diluted drug stocks (180 μL) were added to donor plates (pION INC, Woburn, MA). A filter plate (acceptor plate; pION INC, Woburn, MA) containing 200 μL of acceptor sink buffer (ASB, pH 7.4; pION INC, Woburn, MA) was then placed over the donor plate. The plates were incubated and stirred at room temperature for 0.5 h. Fractions were collected from both the donor plate and the acceptor plate and concentrations were assessed by UV spectrometry (230–500 nm). All compounds were tested in triplicates.

Acknowledgements

This study was supported by the National Institutes of Health grants RC1AI85992, AI057836, AI063054 and the American Lebanese Syrian Associated Charities (ALSAC), St. Jude Children's Research Hospital.

Supplementary data

Supplementary data associated with this article can be found, in the online version, at http://dx.doi.org/10.1016/j.bmc.2013.02.028.

References and notes

1. Lienhardt, C.; Glaziou, P.; Uplekar, M.; Lonnroth, K.; Getahun, H.; Raviglione, M. *Nat. Rev. Microbiol.* **2012**, *10*, 407.
2. Brown, J. R.; North, E. J.; Hurdle, J. G.; Morisseau, C.; Scarborough, J. S.; Sun, D.; Kordulakova, J.; Scherman, M. S.; Jones, V.; Grzegorzewicz, A.; Crew, R. M.; Jackson, M.; McNeil, M. R.; Lee, R. E. *Bioorg. Med. Chem.* **2011**, *19*, 5585.
3. Morisseau, C.; Hammock, B. D. *Annu. Rev. Pharmacol. Toxicol.* **2005**, *45*, 311.
4. Biswal, B. K.; Morisseau, C.; Garen, G.; Cherney, M. M.; Garen, C.; Niu, C.; Hammock, B. D.; James, M. N. *J. Mol. Biol.* **2008**, *381*, 897.
5. Grzegorzewicz, A. E.; Pham, H.; Gundi, V. A. K. B.; Sherman, M. S.; North, E. J.; Hess, T.; Jones, V.; Gruppo, V.; Born, S. E. M.; Kordulakova, J.; Chavadi, S. S.; Morisseau, C.; Lenaerts, A. J.; Lee, R. E.; McNeil, M. R.; Jackson, M. *Nat. Chem. Biol.* **2012**, *8*, 334.
6. Scherman, M. S.; North, E. J.; Jones, V.; Hess, T. N.; Grzegorzewicz, A. E.; Kasagami, T.; Kim, I.-H.; Merzlikin, O.; Lenaerts, A. J.; Lee, R. E.; Jackson, M.; Morisseau, C.; McNeil, M. R. *Bioorg. Med. Chem.* **2012**, *20*, 3255.
7. Bordwell, F. G.; Fried, H. E.; Hughes, D. L.; Lynch, T.-Y.; Satish, A. V.; Whang, Y. E. *J. Org. Chem.* **1990**, *55*, 3330.
8. Yun, M.-K.; Wu, Y.; Li, Z.; Zhao, Y.; Waddell, M. B.; Ferreira, A. M.; Lee, R. E.; Bashford, D.; White, S. W. *Science* **2012**, *335*, 1110.
9. Hurdle, J. G.; Lee, R. B.; Nageshwar, R. B.; Carson, E. I.; Qi, J.; Scherman, M. S.; Cho, S. H.; McNeil, M. R.; Lenaerts, A. J.; Franzblau, S. G.; Meibohm, B.; Lee, R. E. *J. Antimicrob. Chemother.* **2008**, *62*, 1037.
10. Rastogi, N.; Labrousse, V.; Goh, K. S. *Curr. Microbiol.* **1996**, *33*, 167.
11. Meanwell, N. A. *J. Med. Chem.* **2011**, *54*, 2529.
12. Gleeson, M. P. *J. Med. Chem.* **2008**, *51*, 817.
13. Barry, A. L.; Craig, W. A.; Nadler, H.; Reller, L. B.; Sanders, C. C.; Swenson, J. M. *Clin. Lab. Stand. Inst.* **1999**, *19*, M26.
14. Jones, P. D.; Wolf, N. M.; Morisseau, C.; Whetstone, P.; Hock, B.; Hammock, B. D. *Anal. Biochem.* **2005**, *343*, 66.
15. Beetham, J. K.; Tian, T.; Hammock, B. D. *Arch. Biochem. Biophys.* **1993**, *305*, 197.
16. Wixtrom, R. N.; Silva, M. H.; Hammock, B. D. *Anal. Biochem.* **1988**, *169*, 71.
17. Waters, N. J.; Jones, R.; Williams, G.; Sohal, B. *J. Pharm. Sci.* **2008**, *97*, 4586.
18. Di, L.; Kerns, E. H.; Li, S. Q.; Petusky, S. L. *Int. J. Pharm.* **2006**, *317*, 54.
19. Di, L.; Kerns, E. H.; Ma, X. J.; Huang, Y.; Carter, G. T. *Comb. Chem. High Throughput Screening* **2008**, *11*, 469.